Vibrational Energy Transfer from DF(1) to Toluene. Competition between the Benzene Ring CH and Methyl Group CH Stretches

H. K. Shin

Department of Chemistry,† University of Nevada, Reno, Nevada 89557

Received: March 8, 2000; In Final Form: May 24, 2000

Vibrational energy transfer from DF(1) to toluene has been studied by use of the WKB semiclassical procedure in the distorted-wave approximation. Both methyl stretches (ν_4, ν_{17}, ν_{28}) and benzene ring CH stretches (ν_1, ν_2, ν_3) are within 200 cm^{-1} of the DF vibrational frequency. Transfer of this energy mismatch from translation to toluene accompanies the vibration-to-vibration energy exchange step (i.e., VVT). Energy transfer to these two groups of CH modes is treated in both long-range and short-range interactions. At 300 K, the most favored VVT channel is the energy transfer pathway from DF(1) to the ν_4 mode of the methyl CH stretch taking place at long interaction range. The ring CH modes suffer stronger perturbation by DF, but their excitation is not very efficient because they proceed with a larger energy mismatch. However, when the ring mode vibrational frequencies are changed to alter the energy mismatch toward the resonant case, energy transfer to the ring modes at long range becomes the principal energy transfer pathway. The short-range interaction model leads to smaller energy transfer probabilities which vary weakly with the energy mismatch. As temperature increases, probabilities calculated at long range decrease, whereas those calculated at short range increase.

I. Introduction

Gas-phase energy transfer in molecular collisions has been the subject of continuing interest in chemistry and physics for the past several decades.[1−10] The problems of energy transfer rates and mechanisms of diatomic and small polyatomic molecules are, in many respects, well understood. In recent years, collisions involving large organic molecules have been studied actively, revealing valuable information on the rates and the mechanisms of vibrational energy transfer. Large organic molecules can provide a number of near-resonant energy transfer pathways,[11−22] so they are important systems for studying the problem of vibration-to-vibration (VV) energy transfer. Except for the case of exact resonance, intermolecular VV energy transfer involves the energy mismatch ΔE, which has to be transferred to or from other motions such as translation (VT) or rotation (VR). When the magnitude of ΔE is small, the translational motion of the colliding molecules can transfer it efficiently even at long range; i.e., the overall energy transfer process is VVT. Among such collision systems which have been studied are energy transfer between aromatic hydrocarbons and $N_2O(00°1)$ or $CO_2(00°1)$.[11−13,20,21] Normal or deuterated hydrocarbons have their CH stretching frequencies in near resonance with the asymmetric stretch of these triatomic molecules and vibrations of many diatomic species such as DF, CO^+, N_2^+ and OH^+.[23−25] Of these hydrocarbons, toluene has its CH stretching frequencies within 200 cm^{-1} of DF(1). In particular, toluene has two groups of CH stretches (the benzene ring and methyl CH modes) so the collision of this molecule with a vibrationally excited molecule such as DF(1) is a particularly attractive system for studying the competition among the two groups of modes for energy transfer and the mechanism for energy transfer, especially whether it is the short-range repulsive or long-range attractive part of the interaction energy which causes energy transfer.

In this paper, we study the transfer of vibrational energy from DF(1) to the benzene ring CH and methyl CH modes using the WKB semiclassical wave functions in the evaluation of the perturbation integral of the distorted-wave procedure. In this collision, either ring CH or methyl group CH stretches can gain energy from the vibrationally excited DF at short range or long range. The results of this study are interesting from a number of standpoints. In particular, they cast light on the competition between ring CH modes and methyl CH modes in transferring the vibrational energy of DF(1) and the mechanism change for the two groups of modes, especially whether it is the short-range repulsive or long-range attractive interaction which causes intermolecular vibrational energy transfer. The main part of this work is on the energy transfer processes occurring at 300 K. We briefly discuss the temperature dependence of energy transfer probabilities between 100 and 1000 K.

II. Interaction Model and Potential Energies

A. Model and Interatomic Distances. We present the model of interaction between $C_6H_5CH_3$ and DF in Figure 1. To formulate intermolecular potential energies and calculate energy transfer probabilities, we introduce the following approximations:

(1) A rotating DF molecule interacts with a nonrotating toluene molecule. In the interaction region, DF perturbs both methyl CH and adjacent ring CH vibrational motions of toluene. We introduce the angle θ of intersection between the direction of the relative motion and the $H_{ring}-H_{methyl}$ distance to establish the interaction range of DF with *both* methyl CH and adjacent benzene ring CH bonds. We include the interactions of the atoms of DF with the ring H and methyl H in formulating the

† Theoretical Chemistry Group Contribution No. 1171.

10.1021/jp0009094 CCC: $19.00
Published on Web 06/29/2000

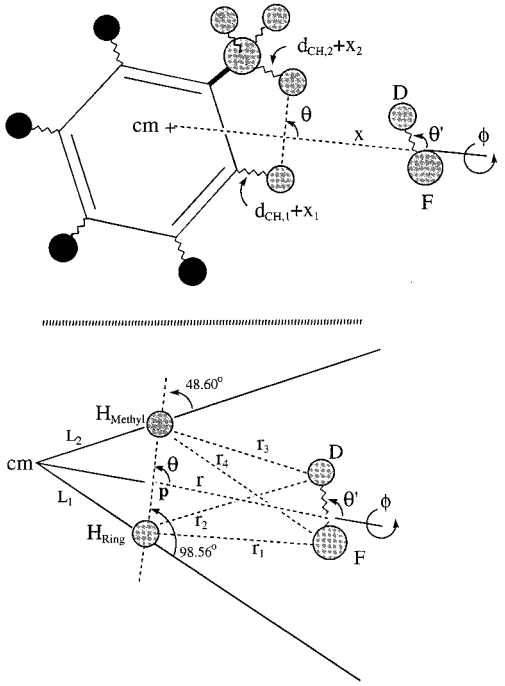

Figure 1. Collision model. The coordinate (x, x_1, x_2, ξ, θ, θ', ϕ) is defined in the upper frame. The atom−atom distances (r_1, r_2, r_3, r_4), the DF-to-p distance r, and the c.m.-to-H distances L_1 and L_2 are defined in the lower frame.

intermolecular potential energy. When DF approaches the center-of-mass (c.m.) of toluene through the ring H atom, the angle θ is 98.56°, where DF is far away from the methyl H. Similarly, when DF approaches toluene in the direction of the methyl H, the angle is 48.60°. In this configuration, DF is now far away from the ring H. We consider the DF-toluene collision which takes place in the segment bound by θ = 48.60° and 98.56°, where *both* groups of CH modes are in interaction with the incident molecule. For DF−toluene collisions taking place outside the region, either methyl H or ring H is too far from DF for effective perturbation to occur. When DF approaches toluene in the direction of bisecting the $H_{ring}-H_{methyl}$ distance, the angle is 69.89°. We consider this bisection configuration to be the representative of the DF-toluene collision in which both groups of CH modes participate in transferring vibrational energy from DF(1).

(2) Energy transfer takes place at molecular separation which is significantly larger than CH and DF bond distances, so that approximate expressions for intermolecular atom−atom distances can be used. These distances will be used to derive the intermolecular potential energy which includes both repulsive and attractive terms in exponential forms as well as the dipole−induced dipole interaction.

(3) In calculating the temperature-dependent energy transfer probability, we will employ the modified wavenumber approximation which will enable us to introduce the impact parameter b by replacing the collision energy E by $E(1 - b^2/b^{*2})$ in the range $0 < b < b^*$, where b^* is chosen such that energy transfer probability is small for $b > b^*$.[26]

The most important step in developing a physically realistic interaction potential model is to use accurate distances between the atoms of the colliding molecules. These distances must have detailed dependence on the pertinent collision coordinates. The interaction energies needed to describe the collision of DF(1) with the ground-state $C_6H_5CH_3$ must contain terms which are responsible for the coupling of the vibrational motion of DF with the ring CH stretch and methyl group CH stretch. The interatomic distances r_1, r_2, r_3 and r_4 are defined in Figure 1. All these distances can be expressed in terms of the coordinates (x_1, x_2, x, ξ, θ, θ', ϕ). Here x is the distance between the c.m. of $C_6H_5CH_3$ and DF describing the relative motion of the collision system and ξ is the displacement of the DF bond distance from its equilibrium value d. x_1 and x_2 are the displacements of the benzene ring CH and methyl CH bond distances from the equilibrium values $d_{CH,1}$ and $d_{CH,2}$, respectively. We note that θ enters in the coordinate system as a parameter defining the direction of approach of DF. We will fix this angle at the representative configuration of 69.89° after discussing the collision characteristics at the high and low ends, 98.56° and 48.60°.

It is convenient to introduce the intersection point p of the $H_{ring}-H_{methyl}$ distance (S) with the direction of the relative coordinate x. We denote the H_{ring}-to-p distance by $\lambda_1 S$ and the H_{methyl}-to-p distance by $\lambda_2 S$, where λ_1 and λ_2 can be explicitly calculated from the collision geometry. Using the methyl CH bond distance $d_{CH,2}$ = 1.091 Å, methyl group C−C−H angle 109.5°, C−C distance 1.530 Å and the ring C-to-toluene c.m. distance 0.940 Å,[27] we find the H_{methyl}-to-toluene c.m. distance L_2 = 3.015 Å. Similarly, using the ring C−H distance $d_{CH,1}$ = 1.084 Å, we find the H_{ring}-to-toluene c.m. distance L_1 = 2.286 Å. From these values, we then obtain $\lambda_1 S = 0.3401 + 2.2600 \cot\theta + 0.1466x_1 + 0.9741 \cot\theta x_1$ and $\lambda_2 S = 1.9953 - 2.2600 \cot\theta + 0.4204x_2 - 0.4762 \cot\theta x_2$, where all distances are expressed in Å. The four atom−atom distances defined in Figure 1 are

$$r_i = [a_i^2 + (-1)^i b_i^2 \cos\phi]^{1/2} \qquad i = 1-4 \tag{1}$$

where

$$a_1^2 = r^2 + \gamma_1^2(d+\xi)^2 + (\lambda_1 S)^2 + 2(\lambda_1 S)r\cos\theta - 2\gamma_1(d+\xi)r\cos\theta'\cos\phi - 2(\lambda_1 S)[\gamma_1(d+\xi)]\cos\theta\cos\theta'\cos\phi$$

$$a_2^2 = r^2 + \gamma_2^2(d+\xi)^2 + (\lambda_1 S)^2 + 2(\lambda_1 S)r\cos\theta + 2\gamma_2(d+\xi)r\cos\theta'\cos\phi + 2(\lambda_1 S)[\gamma_2(d+\xi)]\cos\theta\cos\theta'\cos\phi$$

$$a_3^2 = r^2 + \gamma_2^2(d+\xi)^2 + (\lambda_2 S)^2 - 2(\lambda_2 S)r\cos\theta + 2\gamma_2(d+\xi)r\cos\theta'\cos\phi - 2(\lambda_2 S)[\gamma_2(d+\xi)]\cos\theta\cos\theta'\cos\phi$$

$$a_4^2 = r^2 + \gamma_1^2(d+\xi)^2 + (\lambda_2 S)^2 - 2(\lambda_2 S)r\cos\theta - 2\gamma_1(d+\xi)r\cos\theta'\cos\phi + 2(\lambda_2 S)[\gamma_1(d+\xi)]\cos\theta\cos\theta'\cos\phi$$

$$b_1^2 = 2(\lambda_1 S)[\gamma_1(d+\xi)]\sin\theta\sin\theta'\cos\phi$$

$$b_2^2 = 2(\lambda_1 S)[\gamma_2(d+\xi)]\sin\theta\sin\theta'\cos\phi$$

$$b_3^2 = 2(\lambda_2 S)[\gamma_2(d+\xi)]\sin\theta\sin\theta'\cos\phi$$

$$b_4^2 = 2(\lambda_2 S)[\gamma_1(d+\xi)]\sin\theta\sin\theta'\cos\phi$$

Here $\gamma_1 = m_D/(m_D + m_F)$ and $\gamma_2 = m_F/(m_D + m_F)$. Since the distance from p to the c.m. of toluene is $\sin(\pi - 98.56°)L_1/\sin\theta$, we find $r = x - z = x - (2.2600 + 0.9741x_1)\csc\theta$ in Å. This distance is expressed in terms of the ring CH vibrational displacement, so we use it in obtaining r_1 and r_2. The distance from p to the c.m. is $\sin(48.60°)L_2/\sin(\pi - \theta)$ and the expression of r appropriate for r_3 and r_4 including the methyl CH vibrational coordinate is $r = x - (2.2600 + 0.4762x_2)\csc\theta$.

B. Intermolecular Potential Energies. We introduce the above atom−atom distances in the following interaction potential expressed as a sum of four Morse-type terms and the dipole−induced dipole (DID) energy:

$$U(x_1,x_2,x,\xi,\theta,\theta',\phi) = \sum_{i=1}^{4} D_i[e^{(r_{ie}-r_i)/a_i} - 2e^{(r_{ie}-r_i)/2a_i}] - \alpha\mu^2(3\cos^2\theta' + 1)/(8\pi\epsilon_o x^6) \quad (2)$$

where r_{ie} is the equilibrium value of r_i evaluated at $x_1 = x_2 = \xi = 0$, α is the polarizability of $C_6H_5CH_3$, μ is the dipole moment of DF and ϵ_o is the vacuum permittivity. We consider that the atoms are interacting in the field created by the two molecules, so D and a of the $C_6H_5CH_3$−DF interaction can be used for D_i and a_i in eq 2. Using the combining law for $D_{C_6H_5CH_3} = 377k$[28] and $D_{DF} = 400k$,[29,30] we obtain $D_{C_6H_5CH_3-DF} = 5.36 \times 10^{-14}$ erg. We note that the DF−DF hydrogen-bond energy is as large as 6 kcal/mol or 4.17×10^{-13} erg,[31] but use of such a large value is not appropriate for the gas-phase interaction between DF and a saturated hydrocarbon. We expect the range parameter a for $C_6H_5CH_3$−DF to be significantly larger than 0.20−0.25 Å, the values that have often been used for simple molecular systems.[6,32] In fact, we have used $a = 0.34$ Å for $C_6H_5CH_3$−N_2O.[21] Since the values of a for both DF and N_2O are close to 0.20 Å,[20,21,29] we choose the same magnitude of 0.34 Å for the present system. When we use the polarizability of 13 Å^3 estimated for toluene[28] and the dipole moment of 1.82D for DF,[27] the dipole−induced dipole energy is $U_{DID} = -2.15 \times 10^{-11}(3\cos\theta' + 1)/x^6$ in erg, where x is in Å. With the Lennard-Jones (LJ) parameters $\sigma_{C_6H_5CH_3} = 5.932$ Å and $\sigma_{DF} = 3.0$ Å,[28−30] we obtain the combining-law result $\sigma_{C_6H_5CH_3-DF} = 4.47$ Å. Using this value, we can estimate the equilibrium distance $x_{e,LJ} = 2^{1/6}\sigma_{C_6H_5CH_3-DF} = 5.01$ Å. We then make the orientation average of the interaction including the DID term as discussed below and recalculate the equilibrium distance for a fixed value θ. At the distance 5.01 Å, the orientation-averaged DID energy is -2.75×10^{-15} erg. This value is very small compared with $D_{C_6H_5CH_3-DF} = 5.36 \times 10^{-14}$ erg as well as $kT = 4.14 \times 10^{-14}$ erg at 300 K. The main effect of the DID term in eq 2 is to deepen the potential well by a small extent. This effect can be accounted for by converting the power x^{-6} to an exponential form as $x^{-6} = x_e^{-6}(1 - b\ln y)^{-6} = 1 + 6b\ln y + 21b^2\ln^2 y + 56b^3\ln^3 y + ...$, where $y = e^{(x_e-x)/2a}$ and $b = 2a/x_e$. For $2 > y > 0$, $\ln y = (y-1) + {}^1/_2(y-1)^2 + {}^1/_3(y-1)^3 + ...$ Sample calculations show that energy transfer probabilities obtained in this procedure are very close to a simpler approach which uses the DID term evaluated at x_e. We employ the latter procedure.

In the range of $\theta = 48.60°$ and 98.56°, cot θ varies from 0.8816 to −0.1505. At the bisection point $\theta = 69.89°$, cot θ is 0.3661. Since r is typically 3−4 Å, which is significantly larger than $\gamma_1(d+\xi)$, $\gamma_2(d+\xi)$, $\lambda_1 S$ and $\lambda_2 S$, we can write eq 1 in the form $r_i = r[(a_i/r)^2 + (-1)^i(b_i/r)^2\cos\phi]^{1/2}$ and expand the terms in the radical in a power series of $1/r$. In the expansion, higher-order terms ($1/r^2$ and higher) are mainly responsible in modifying the interaction potential well and energies at long range, so we take their values at the equilibrium separation. When all numerical factors are explicitly calculated, the atom−atom distance r_1 appropriate for the present energy transfer process can be obtained in the lengthy but rigorous expression

$$r_1 = x + [0.0123 - 2.2600\csc\theta + 0.3400\cos\theta + (0.1537 + 2.2604\cos\theta)\cot\theta + 0.5109\cot^2\theta - 0.0878\cos\theta'\cos\phi - (0.0060 + 0.0397\cot\theta)\times(\cos\theta\cos\theta'\cos\phi + \sin\theta\sin\theta'\cos\phi)] + [0.0100 - 0.9741\csc\theta + 0.1325\cot\theta + 0.4403\cot^2\theta + 0.1466\cos\theta + 0.9741\cos\theta\cot\theta - (0.0026 + 0.0171\cot\theta)(\cos\theta\cos\theta'\cos\phi + \sin\theta\sin\theta'\cos\phi)]x_1 + [0.0017 - 0.958\cos\theta'\cos\phi - (0.0065 + 0.0433\cot\theta)\times(\cos\theta\cos\theta'\cos\phi + \sin\theta\sin\theta'\cos\theta)]\xi - [(0.0028 + 0.0187\cot\theta)(\cos\theta\cos\theta'\cos\phi + \sin\theta\sin\theta'\cos\phi)]x_1\xi \quad \text{(in Å)} \quad (3)$$

Distances r_2, r_3 and r_4 can be obtained in similar expressions. In eq 3, the terms in the first brackets are independent of vibrational coordinates x_1, x_2 and ξ. Thus, we define r_{1e} as the θ', ϕ-average of r_1 at $x = x_e$ and $x_1 = x_2 = \xi = 0$ for a given value of θ. For the representative configuration $\theta = 69.89°$, $r_{1e} = 1.868$ Å, $r_{2e} = 1.800$ Å, $r_{3e} = 2.725$ Å and $r_{4e} = 2.783$ Å. In deriving the interaction potential energy, we expand the x_1, x_2 and ξ dependent terms in each exponent and write the repulsive term in the form

$$De^{(r_{1e}-r_1)/a} = De^{(x_e-x)/a}e^{f_1(\theta,\theta',\phi)/a}[1 + g_1(\theta,\theta',\phi)(x_1\xi/a^2)] \quad (4)$$

where $f_1(\theta,\theta',\phi)$ is the terms in the first brackets of eq 3 and $g_1(\theta,\theta',\phi)$ is the sum of x_1, ξ and $x_1\xi$-dependent terms in the expansion of $e^{(r_{1e}-r_1)/a}$. We retain all expanded terms containing $x_1\xi$ in eq 4. The other exponential terms can be expressed similarly. We note that while $e^{(r_{1e}-r_1)/a}$ and $e^{(r_{2e}-r_2)/a}$ contain $x_1\xi$-dependent terms, $e^{(r_{3e}-r_3)/a}$ and $e^{(r_{4e}-r_4)/a}$ contain $x_2\xi$-dependent terms. The attractive energy term $2De^{(r_{1e}-r_1)/2a}$ appearing in eq 2 takes the same form as eq 4 except that a is now replaced by $2a$. When we introduce these repulsive and attractive terms in the four atom−atom interactions of eq 2, the interaction potential energy can be written in the form

$$U(x_1,x_2,x,\xi,\theta,\theta',\phi) = D[A(\theta,\theta',\phi)e^{(x_e-x)/a} - 2B(\theta,\theta',\phi)e^{(x_e-x)/2a} + U_{DID}(x,\theta')] + D[A_1'(\theta,\theta',\phi)e^{(x_e-x)/a} - 2B_1'(\theta,\theta',\phi)e^{(x_e-x)/a}](x_1\xi/a^2) + D[A_2'(\theta,\theta',\phi)e^{(x_e-x)/a} - 2B_2'(\theta,\theta',\phi)e^{(x_e-x)/a}](x_2\xi/a^2) \quad (5)$$

where $A(\theta,\theta',\phi) = \sum_{i=1}^{4} e^{f_i(\theta,\theta',\phi)/a}$, $A_1'(\theta,\theta',\phi) = \sum_{i=1}^{2} g_i(\theta,\theta',\phi)e^{f_i(\theta,\theta',\phi)/a}$ and $A_2'(\theta,\theta',\phi) = \sum_{i=3}^{4} g_i(\theta,\theta',\phi)e^{f_i(\theta,\theta',\phi)/a}$. The expressions of $B(\theta,\theta',\phi)$, $B_1'(\theta,\theta',\phi)$ and $B_2'(\theta,\theta',\phi)$ are the same as the corresponding repulsive terms except that a is now replaced by $2a$.

To complete the excitation of the toluene CH mode, the process of energy transfer from DF(1) to toluene must be accompanied by the transfer of ΔE from translation to the toluene vibration. We do not consider rotational energy transfer in the present collision. In the related systems of p-$C_6H_4F_2$ with H_2, D_2, and N_2 (where the organic molecule is in an excited state) Mudjijono and Lawrance have shown that there is no evidence of VR energy transfer.[16] However, in such collisions involving a large target molecule, the orientation of the incident molecule can significantly affect interaction energies. The orientation effect can be particularly important in toluene where two different groups of CH modes compete for energy transfer.

TABLE 1: θ', ϕ-Averaged Interaction Energy Coefficients at Various θ

θ, deg	$A(\theta)$	$B(\theta)$	$A_1'(\theta)$	$B_1'(\theta)$	$A_2'(\theta)$	$B_2'(\theta)$
48.60	6.119	4.406	0.4403	0.0345	0.2603	0.0072
69.89	5.418	4.294	0.4316	0.0231	0.1732	0.0039
98.56	5.732	4.346	0.3178	0.0088	0.1833	0.0142

A reasonable approach to account for this effect is averaging eq 5 over θ' from 0 to π and ϕ from 0 to 2π:

$$U(x_1,x_2,x,\xi,\theta) = D[A(\theta)e^{(x_e-x)/a} - 2B(\theta)e^{(x_e-x)/2a} + U_{DID}(x)] + D[A_1'(\theta)e^{(x_e-x)/a} - 2B_1'(\theta)e^{(x_e-x)/a}](x_1\xi/a^2) + D[A_2'(\theta)e^{(x_e-x)/a} - 2B_2'(\theta)e^{(x_e-x)/a}](x_2\xi/a^2)$$
$$= U_0(x,\theta) + \bar{U}_1'(x,\theta)(x_1\xi/a^2) + \bar{U}_2'(x,\theta)(x_2\xi/a^2) \quad (6)$$

where $A(\theta)$, $B(\theta)$, $A'(\theta)$ and $B'(\theta)$ are the θ', ϕ-average of the corresponding coefficients defined in eq 5. The perturbation term $\bar{U}_1'(x,\theta)(x_1\xi/a^2)$ is responsible for inducing energy transfer to the ring CH stretches, whereas $\bar{U}_2'(x,\theta)(x_2\xi/a^2)$ is responsible for energy transfer to the methyl CH stretches. Here we group a^2 with the vibrational coordinates to make the factor dimensionless. There is no natural way of averaging the interaction energy over θ', which is considered to vary between the lower end 48.60° and the upper end 98.56°. Thus, we treat the collision at these two angles individually to establish energy transfer characteristics at each end and then treat the case of the representative configuration ($\theta = 69.89°$) in detail. In Table 1, we list the θ', ϕ-averaged $A(\theta)$, $B(\theta)$, $A'(\theta)$ and $B'(\theta)$ at these three θ values.

In Figure 2, we plot θ', ϕ-dependent potential energy $U_o(x,\theta,\theta',\phi)$ and the θ', ϕ-averaged energy at $\theta = 69.86°$ to gauge their general characteristics. The minimum of the Morse-DID intermolecular potential lies between 5 and 6 Å, which is in the correct range of collision systems involving a large aromatic hydrocarbon. The combination of the attractive terms of the Morse function and the DID terms emphasizes the importance of molecular attraction. We can include still higher order terms such as the attractive energy from dipole−quadrupole interaction, but the Morse and DID terms exert the dominant influence on energy transfer. As shown in Figure 2, where $\theta' = 180°$ and $\phi = 0°$, the equilibrium separation is as large as 5.74 Å. At this linear configuration, the D end of the incident molecule is oriented toward two H atoms, so the c.m. of DF is farther away from toluene. When $\theta' = 0°$ and $\phi = 0°$, the F end is now near the H atoms and the c.m. of DF is closer to toluene. For this configuration, the equilibrium separation is only 4.99 Å. The $\theta' = \phi = 90°$ case, in which DF is aligned perpendicular to the molecular plane of toluene, the equilibrium separation lies between the above two linear configurations with a significantly deeper well-depth. It is interesting to note that the equilibrium separation for this perpendicular case is 5.01 Å, which is identical to the LJ distance $x_{e,LJ}$ estimated above. For the θ',ϕ-averaged potential, which will be used below, the equilibrium distance is 5.17 Å, which is somewhat larger than the LJ value (see Figure 2). Both equilibrium separation and well depth for this averaged potential energy lie between all these θ',ϕ-dependent cases considered in Figure 2. A more rigorous approach to the interaction model is to use a full dimensional potential energy surface based on ab initio calculations. However, such calculations do not appear possible at present for collisions involving large molecules. Until such a PES becomes available, the present procedure of formulating the exponential interactions in terms of rigorously determined atom−atom distances and long-range attractions is of practical value in handling such collision systems.

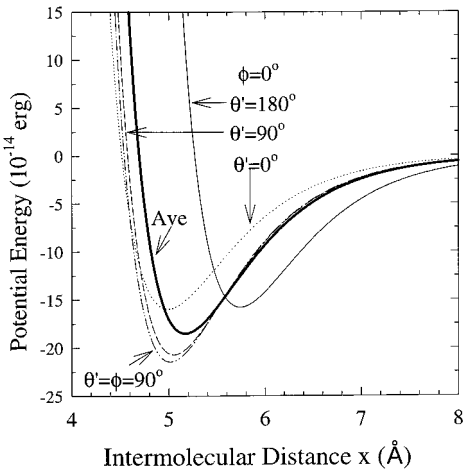

Figure 2. Intermolecular potential energies at various orientations (θ' and ϕ) for the representative configuration $\theta = 68.89°$. The heavy curve represents the θ', ϕ-averaged potential energy.

III. Energy Transfer to CH Stretch Modes

A. Energy Transfer Probability. For the collision-induced i → f transition, the probability can be given in the distorted-wave approximation by[33−35]

$$P_{if}(E) = \frac{8m}{\hbar^2(E_iE_f)^{1/2}}\left|\int_{x_l}^{x_u}\psi_f(E_f,x)[\bar{U}_1'(x,\theta)\langle f|x_1\xi/a^2|i\rangle + \bar{U}_2'(x,\theta)\langle f|x_2\xi/a^2|i\rangle]\psi_i(E_i,x)\,dx\right|^2 \quad (7)$$

where $E_i = E$, the initial collision energy, and E_f is the final energy ($E + \Delta E$). For a given value of θ, the integral contains two perturbation integrals $F_{if,1} = \int_{x_l}^{x_u}\psi_f(E_f,x)\,\bar{U}_1'(x,\theta)\,\psi_i(E_i,x)\,dx$ and $F_{if,2} = \int_{x_l}^{x_u}\psi_f(E_f,x)\,\bar{U}_2'(x,\theta)\,\psi_i(E_i,x)\,dx$, which we now evaluate using the WKB wave functions[36,37]

$$\psi_{i,f}(E_{i,f},x) = \frac{1}{2}[k(E_{i,f})/k(E_{i,f},x)]^{1/2} \times \exp\left\{\pm\frac{(2m)^{1/2}}{\hbar}\int_{x_{t,i,f}}^{x}[\bar{U}_0(x,\theta) - E_{i,f}]\,dx\right\} \quad \text{for } x < x_{t,i,f} \quad (8)$$

$$\psi_{i,f}(E_{i,f},x) = [k(E_{i,f})/k^*(E_{i,f},x)]^{1/2} \times \cos\left\{\frac{(2m)^{1/2}}{\hbar}\int_{x_{t,i,f}}^{x}[E_{i,f} - \bar{U}_0(x,\theta)]\,dx\right\} \quad \text{for } x > x_{t,i,f} \quad (9)$$

where $k(E_i) = (2mE)^{1/2}/\hbar$, $k(E_f) = [2m(E + \Delta E)]^{1/2}/\hbar$, $k(E_i,x) = \{2m[\bar{U}_0(x,\theta) - E]\}^{1/2}/\hbar$, $k(E_f,x) = \{2m[\bar{U}_0(x,\theta) - (E + \Delta E)]\}^{1/2}/\hbar$, m is the reduced mass of the collision system and x_t's are the turning points ($x_{t,i}$ and $x_{t,f}$). In the cosine functions for $x > x_{t,i,f}$, $k^*(E_i,x) = \{2m[E - \bar{U}_0(x,\theta)]\}^{1/2}/\hbar$ and $k^*(E_f,x) = \{2m[(E + \Delta E) - \bar{U}_0(x,\theta)]\}^{1/2}/\hbar$. The integrals in the exponent are table integrals, which can be readily evaluated. Such WKB wave functions have been used in the evaluation of the perturbation integral F_{if} that appears in the quantum mechanical treatment of molecular interactions.[20,21,36−43] Equation 8 describes the collisions at short-range ($x < x_t$), where repulsive interactions are of major importance, whereas eq 9 is appropriate for the collision taking place at long range ($x > x_t$), where the attractive part of the intermolecular potential causes vibrational

energy to be transferred. Thus, throughout in this paper, we shall refer to the use of these two equations in the evaluation of the perturbation integrals as the short-range and long-range interaction models, respectively. The vibrational matrix element $\langle f|x_1\xi/a^2|i\rangle$ determines the efficiency of VV energy exchange. In the VV exchange, the vibrational state of DF changes from $\nu_{DF} = 1$ to 0, while that of toluene changes from $\nu_{CH} = 0$ to 1 so the matrix element is the product of two factors, $\langle 0|x_1/a|1\rangle \cdot \langle 1|\xi/a|0\rangle$. In the harmonic oscillator model for the vibrations of DF and toluene, the matrix element is $\langle f|x_1\xi/a^2|i\rangle = (\hbar/2m_{CH,1}\omega_{CH,1})^{1/2}(\hbar/2m_{DF}\omega_{DF})^{1/2}/a^2$, where $m_{CH,1}$ is the reduced mass of CH associated with the ring CH stretch and m_{DF} is the reduced mass of DF. The ring-stretch and DF frequencies are denoted by $\omega_{CH,1}$ and ω_{DF}, respectively. Similarly, the matrix element for energy transfer to the methyl CH mode is $\langle f|x_2\xi/a^2|i\rangle = (\hbar/2m_{CH,2}\omega_{CH,2})^{1/2}\,(\hbar/2m_{DF}\omega_{DF})^{1/2}/a^2$, where $m_{CH,2}$ is the reduced mass of CH associated with the methyl CH stretch and $\omega_{CH,2}$ is the methyl CH stretch frequency.

To calculate the temperature-dependent energy transfer probability $P(T)$, we average eq 6 over the Boltzmann distribution of collision energies and integrate over the impact parameter b after replacing E in $P_{if}(E)$ by $E(1 - b^2/b^{*2})$ in the range of $0 < b < b^*$. With this replacement, we now have the probability as a function of both E and b, $P_{if}(E,b)$, which can be integrated over E and b to derive

$$P(T) = \frac{8m}{\hbar^2[E(E+\Delta E)]^{1/2}\pi b^{*2}}\int_0^{b^*} 2\pi b\, db \int_{E_l}^{\infty} E e^{-E/kT} \times dE\{\int_{x_l}^{x_u}\psi_f(E_f,x)[\langle f|x_1\xi/a^2|i\rangle \bar{U}_1'(x,\theta) + \langle f|x_2\xi/a^2|i\rangle \bar{U}_2'(x,\theta)]\psi_i(E_i,x)\, dx\}^2 \quad (10)$$

where the lower limit E_l of the E-integration is zero for exoergic energy transfer processes ($\Delta E \geq 0$) and is $|\Delta E|$ for endoergic processes ($\Delta E \leq 0$). The combined process of VV energy exchange between DF(1) and the ground state toluene and VT transfer from translation to toluene can take place at long or short range of interaction. While the VV exchange is very efficient, the VT step can be inefficient if the energy mismatch is large. The efficiency of the overall energy transfer process can vary significantly whether the process is taking place at long range or short range.

In the long-range interaction model, we evaluate the perturbation integrals $F_{if,1}$ and $F_{if,2}$, which are the x-integrals, from $x = +\infty$ to x_u, where the upper limit x_u lies just outside the turning point $x_{t,i}$, covering the entire region of molecular attraction. This limit will be determined numerically (see below). We note that in the narrow segment $x_u < x \leq x_0$, where x_0 is the potential-zero distance determined from $\bar{U}_0(x_0,\theta) = 0$, the interaction is slightly repulsive.

In the short-range interaction model, DF approaches within close range of the target, where repulsive interactions are of major importance, for VVT energy transfer. When ΔE is small, the integrands in the exponent of eq 8 for the initial and final wave functions differ only slightly from each other, so an accurate evaluation of the x-integral in eq 10 is essential. We carry out the x-integration from $x = x_{t,i}$ to x_u, where the upper limit is now a distance inside the turning $x_{t,f}$. The extent of barrier penetration becomes particularly important when the energy mismatch is large. We will determine the upper limit numerically in the following sections. To appreciate the need of a numerical procedure for determining x_u in both short and long-range interactions, we note the complicated form of the perturbation integrals shown in the Appendix. In eq A1, we have transformed the x-integration of $F_{if,1}$ to the y-integral using the transformation $y = e^{(x_e - x)/2a}$ so the upper limit is now $y_u = e^{(x_e - x_u)/2a}$. Because of singularities and imaginary numbers, the derivation of an explicit form of the upper limit, which must satisfy the condition $y_u > B(\theta)/A(\theta) + \{B(\theta)^2 + A(\theta)[E(1 - b^2/b^{*2}) + \Delta E + U_{DID}]/D\}^{1/2}/A(\theta)$, is not possible. The desired limit is the smallest value of y_u satisfying this condition. The best way to find y_u is to carry out the triple integration of eq 10 for a series of y values inside the turning $y_{t,f} = e^{(x_e - x_{t,f})/2a}$ for the E-integration from E_l to $+\infty$ and the b-integration from 0 to b^*. A similar procedure needs to be used to determine the upper limit y_u of the y-integral for the long-range interaction model. The y-integral for this model is given by eq A2.

The vibrational motions of toluene in which we are interested are the ν_4, ν_{17} and ν_{28} modes of the methyl group CH stretches, and ν_3, ν_2 and ν_1 modes of the CH stretches on the benzene ring. When we use the designations of modes adopted in ref 44, the energy transfer processes for the methyl modes are

$$C_6H_5CH_3(\nu_4{=}0) + DF(1) \rightarrow C_6H_5CH_3(\nu_4{*}) + DF(0) + \Delta E = -14\ cm^{-1}$$

$$C_6H_5CH_3(\nu_{28}{=}0) + DF(1) \rightarrow C_6H_5CH_3(\nu_{28}{*}) + DF(0) + \Delta E = -45\ cm^{-1}$$

$$C_6H_5CH_3(\nu_{17}{=}0) + DF(1) \rightarrow C_6H_5CH_3(\nu_{17}{*}) + DF(0) + \Delta E = -72\ cm^{-1}$$

For the three ring modes, the processes are

$$C_6H_5CH_3(\nu_3{=}0) + DF(1) \rightarrow C_6H_5CH_3(\nu_3{*}) + DF(0) + \Delta E = -147\ cm^{-1}$$

$$C_6H_5CH_3(\nu_2{=}0) + DF(1) \rightarrow C_6H_5CH_3(\nu_2{*}) + DF(0) + \Delta E = -156\ cm^{-1}$$

$$C_6H_5CH_3(\nu_1{=}0) + DF(1) \rightarrow C_6H_5CH_3(\nu_1{*}) + DF(0) + \Delta E = -178\ cm^{-1}$$

Here the asterisk represents the vibrationally excited mode of toluene by one quantum. The energy mismatch ΔE is the difference between 2907 cm^{-1} for DF(1) and the value of the collisionally excited mode in toluene.

As shown in Figure 1, at $\theta = 48.60$ °, DF approaches the c.m. of toluene through the methyl H atom, whereas at $\theta = 98.56$ °, it approaches the c.m. through the ring H atom. We note that the equilibrium separation between DF and the c.m. of toluene is ~5 Å. Since the methyl H is about 3 Å away from the c.m. of toluene, DF approaching the methyl H side of toluene with less than 48.60° will not significantly perturb the distant ring CH vibration. Similarly, DF approaching the ring H side of toluene with $\theta > 98.56°$ will not produce any significant perturbation to the distant methyl CH vibration. Thus, these angles introduce a natural region of interaction, where the transfer of vibrational energy from DF(1) to both methyl and ring CH stretches can occur to a significant extent.

B. $\theta = 48.60°$. We first consider energy transfer to the CH modes at the lower angle $\theta = 48.60°$ at 300 K. In this configuration, DF can produce a strong disturbance to the nearby methyl CH vibration so energy transfer to its modes can take place efficiently. In Figure 3a, we show energy transfer probabilities for all six processes as a function of the energy mismatch, ΔE, calculated in the short and long-range interaction models. (For convenience we use the magnitude $|\Delta E|$.) The numerical values of energy transfer probabilities for this and

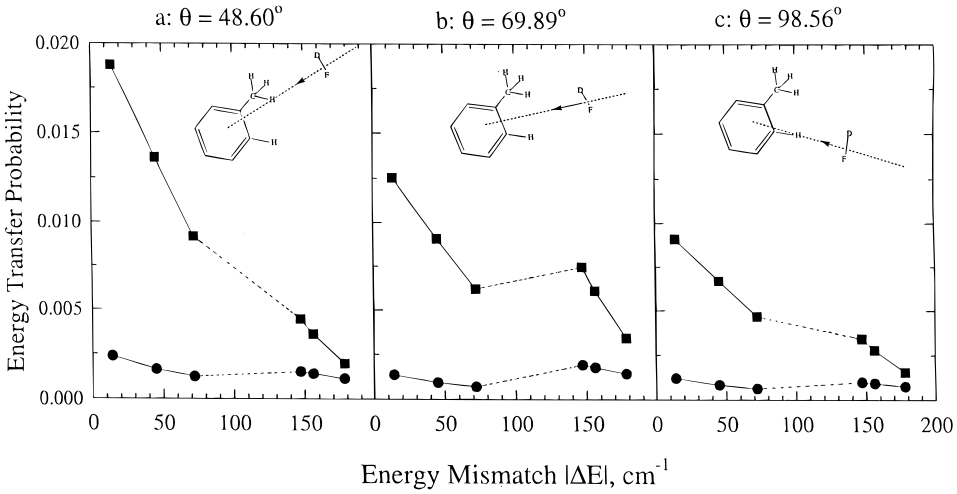

Figure 3. Variation of energy transfer probabilities with energy mismatch at 300 K for = 48.60°, 69.89°, and 98.56°. The sketch of each collision configuration is shown. In each figure, the upper and lower curves are the results of collisions taking place at long range and short range, respectively. The points at $|\Delta E| = 14$, 45, and 72 cm^{-1} are for the methyl CH modes and those at $|\Delta E| = 147$, 156, and 178 cm^{-1} are for the benzene ring CH modes. Two groups are connected by a dotted line for easy comparison.

TABLE 2: Energy Transfer Probabilities at 300 K

	$\theta = 48.60°$		$\theta = 69.89°$		$\theta = 98.56°$	
	long-range	short-range	long-range	short-range	long-range	short-range
			Methyl CH Modes			
ν_4	0.0188	0.00238	0.0125	0.00137	0.00908	0.00121
ν_{28}	0.0136	0.00165	0.00909	0.000942	0.00670	0.000836
ν_{17}	0.00917	0.00125	0.00620	0.000708	0.00467	0.000632
			Ring CH Modes			
ν_3	0.00446	0.00152	0.00746	0.00194	0.00342	0.00100
ν_2	0.00362	0.00141	0.00611	0.00179	0.00278	0.000926
ν_1	0.00198	0.00114	0.00343	0.00145	0.00155	0.000750

two other θ are summarized in Table 2. The vibrational excitation of the ν_4 methyl CH stretching mode, which is in near resonance with the DF vibration, is very efficient at long range. The energy transfer probability for this mode is as large as 0.0188. The long-range probability decreases as the energy mismatch increases. For the ν_{28} and ν_{17} modes of the methyl CH stretches, for which $\Delta E = -45$ and -72 cm^{-1}, respectively, the energy transfer probability decreases to 0.0136 and 0.00917. As shown in Table 1, the perturbation coefficients $A_1'(\theta)$ and $B_1'(\theta)$ for the ring CH vibration are nearly twice those of the methyl CH vibration, $A_2'(\theta)$ and $B_2'(\theta)$, but the ring CH is farther away from the DF as determined by the exponential factors $e^{(x_e-x)/a}$ and $e^{(x_e-x)/2a}$ in eq 6, causing $\bar{U}_2'(x,\theta)$ to be significantly smaller than $\bar{U}_1'(x,\theta)$. For the ν_3, ν_2 and ν_1 ring CH modes with $\Delta E = -147$, -156 and -178 cm^{-1}, respectively, energy transfer probabilities at 300 K are only 0.00446, 0.00362, and 0.00198. The energy transfer probabilities displayed in Figure 3a for θ = 48.60° clearly indicate the dominance of the methyl CH modes in transferring vibrational energy from DF(1) in long-range interactions.

When the short-range collision model is invoked, the energy transfer probabilities of all six modes are very small ($\approx 10^{-3}$) and they exhibit a weak dependence on the energy mismatch. In fact, the probabilities of ν_4 excitation ($\Delta E = -14$ cm^{-1}) and ν_3 excitation $\Delta E = -147$ cm^{-1}) differ only slightly, even though there is a 10-fold change in ΔE. When the energy mismatch increases, the translational motion has to supply a greater amount of energy, but this VT step is not very efficient. However, this inefficiency is largely offset by greater perturbation energy for the ring modes (see Table 1) in short-range interactions, so the net change between the methyl and ring mode probabilities is not very significant as shown in Figure 3a. In the short-range

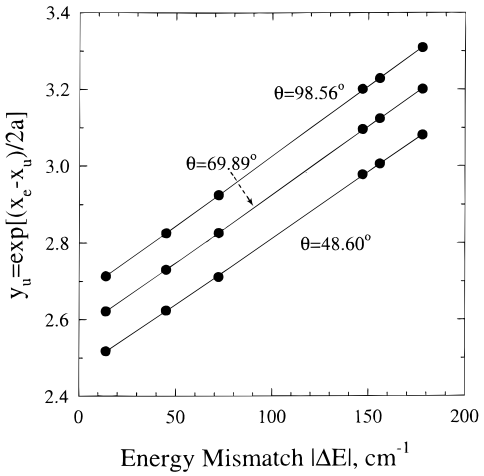

Figure 4. Variation of the upper limit of the *y*-integration in the short-range interaction mode with energy mismatch.

model, when the energy mismatch is large, the colliding molecules must approach within close range of each other to transfer ΔE, i.e., a repulsive region farther away from the turning point $x_{t,f}$. This situation corresponds to $y_u = e^{(x_e-x_u)/2a}$ taking a larger value, which leads to a larger value of the perturbation integrals. The rising y_u tends to increase the magnitude of the *y*-integral, but the increasing ΔE counters the effect, thus resulting in energy transfer probabilities which change only slightly with ΔE. For the ν_3 excitation, for example, the upper limit y_u of the *y*-integral in eq A1 is 2.517. Thus, the θ', ϕ-averaged interaction energy for θ = 48.60° in this limit is $\bar{U}_0(x_u,\theta) = D[A(\theta)e^{(x_e-x_u)/a} - 2B(\theta)e^{(x_e-x_u)/2a}] + U_{DID} = 8.92 \times 10^{-13}$ erg, which lies in the repulsive interaction region. As shown in Figure 4, this upper limit of the y-integration rises linearly with increasing energy mismatch. The lowest line is for the θ = 48.60° configuration and other lines are for the cases considered below.

C. θ = 98.56°. As shown in Figure 3c and Table 2, the variation of energy transfer probabilities with the energy mismatch is qualitatively similar to that of the $\theta = 48.60°$ case. The long-range interaction model still produces larger probabilities for the methyl CH modes than the ring modes. The probability of energy transfer to the ν_4 methyl mode is 0.00908, the largest of all six probabilities, though it is only about half

the value of the $\theta = 48.60°$ configuration. However, energy transfer probabilities for the two different CH groups in this configuration are not greatly different. In fact, the probability of energy transfer to the ν_{17} methyl mode is only slightly larger than that to the ν_3 ring mode (0.00467 versus 0.00342). Thus, although long-range interactions are no longer as efficient as those in the smaller angle θ case considered in the previous section, they still produce main energy transfer pathways for receiving vibrational energy from DF(1).

Energy transfer probabilities calculated in the short-range interaction model are small ($\approx 10^{-3}$) and vary only slightly over the entire range of $|\Delta E|$ from 14 cm^{-1} of the methyl CH to 178 cm^{-1} of the ring CH. This is mainly due to the compensation of the contribution of stronger short-range interactions (i.e., larger *y*-integral) by the inefficiency of transferring a larger amount of the energy mismatch. We note that the probability of the ν_3 ring mode excitation is now larger than the ν_{17} methyl mode probability (0.00100 versus 0.000632), despite the energy mismatch for the former process doubling that of the latter.

When $\theta = 98.56°$, the incident molecule is now close to the ring CH bond, causing a stronger perturbation to the ν_3, ν_2 and ν_1 ring CH modes than to the modes of the distant methyl CH (see Table 1). As shown in Figure 3c and Table 2, energy transfer probabilities for the methyl CH modes are smaller compared with the $\theta = 48.60°$ case as expected. An interesting result shown in Table 2 is that the ring CH mode probabilities for $\theta = 98.56°$ are likewise smaller, even though DF approaches the ring H side. In the $\theta = 98.56°$ case, the incident molecule now has to approach the "hard-core" region of the ring to interact with the CH stretching modes, but this region is not readily accessible to DF. As shown in section IIA, the H_{ring}-to-toluene c.m. distance L_1 is 2.286 Å, which is much shorter than $L_2 = 3.015$ Å for the H_{methyl}-to-toluene distance and represents a strongly repulsive region. Thus, it is difficult for DF to approach close proximity of the ring CH bond in this direction and produce a strong perturbation in the ring CH. Consequently, the perturbation energy coefficient $A_1'(\theta)$ and $B_1'(\theta)$ for this configuration are smaller than those of $\theta = 48.60°$ (see Table 1) and they result in smaller probabilities. For example, the ν_3 probability decreases to 0.0010 at $\theta = 98.56°$ from 0.0015 at $\theta = 48.60°$. Note that in the short-range interaction model, energy transfer probabilities increase with rising temperatures as more molecules can approach in the "hard-core" interaction region. This aspect of the temperature dependence will be discussed in section IV.

D. $\theta = 69.89°$. The above results indicate that the principal pathway at the upper and lower ends of θ is near-resonant energy transfer to the ν_4 methyl CH mode at long range. To examine the details of individual energy transfer pathways when DF interacts with both groups of CH modes at the same distance, we now take the representative configuration ($\theta = 69.89°$). We plot energy transfer probabilities for this configuration in Figure 3b and compare the result with those of the previous two configurations shown in Figure 3a,c (also see Table 2). The activation of the ν_4 methyl CH mode in the long-range model is still the most efficient transfer pathway. As shown in Figure 3b, the probabilities for the methyl modes calculated at this representative configuration in the long-range interaction model lies between those values of the $\theta = 48.60°$ and 98.56° cases as expected. For example, the ν_4 methyl mode probabilities are 0.0188, 0.0125, and 0.00908 for $\theta = 48.60°$, 69.89° and 98.56°, respectively.

We know of no specific result, either experimental or theoretical, which can be compared directly with the energy transfer probabilities obtained in the present work. However, the present values calculated in the long-range interaction model are comparable to the deactivation probabilities of $N_2O(00°1)$ or $CO_2(00°1)$ by a number of aromatic hydrocarbons and their fluorine derivatives for which the values of ΔE are similar to those of the present system.[11−13,21] For example, the observed probability of the deactivation of $N_2O(00°1)$ by toluene at room temperature is 0.00708.[12] In $C_6D_5CD_3(\nu_i=0) + N_2O(00°1) \rightarrow C_6D_5CD_3(\nu_i*) + N_2O(00°0)$, which has five near-resonant channels ($\Delta E = +1, +8, -38, -36, -62$ cm^{-1}) involving $\Delta v = 2$, the observed probability at 295 K is 0.0230.[12] Here $\Delta E = +1$ cm^{-1} is for the methyl group CD stretch ν''_a mode. On the other hand, the observed probability for $C_6D_6(\nu_i=0) + N_2O(00°1) \rightarrow C_6D_6(\nu_i*) + N_2O(00°0)$ with $\Delta E = -43, -63, -68, -69$ cm^{-1}, also involving two quantum number changes, the observed probability is 0.0125.[12] Thus, the ratio of the observed toluene probability to the observed benzene probability is 0.0230/0.0125 = 1.84, which is the relative efficiency of energy transfer processes with and without the methyl group as in the present study. Although the collisions are different, therefore, the comparison of this ratio to that of the methyl CH mode probability to the benzene ring CH mode probability in the present study should be interesting. In the present study, the corresponding ratio for the largest methyl CH probability (ν_4 mode) to the largest ring CH probability (ν_3 mode) in the long-range interaction model is 0.0125/0.00746 = 1.68, which is close to the observed ratio for the deuterated hydrocarbon−N_2O systems. We note that in $C_6D_5CD_3(\nu_i=0) + N_2O(00°1)$ the observed probability of 0.0125 is most likely due to the near perfect match between the ν''_a CD antisymmetric stretch of the methyl group in $C_6D_5CD_3$ at 2223 cm^{-1} and the ν_3 stretch mode of N_2O at 2224 cm^{-1}($\Delta E = +1$ cm^{-1}). Therefore, if we assume $\Delta E = +1$ cm^{-1} for the methyl CH mode in the present $C_6H_5CH_3(\nu_i=0) + DF(1)$ collision instead of $\Delta E = -14$ cm^{-1} for the ν_4 mode, the resulting probability in the long-range interaction is 0.0140. Then the probability ratio is 0.0140/0.00746 = 1.88, which is closer to the observed ratio of 1.84 for the deuterated systems. This comparison supports the usefulness of the present approach in studying vibrational energy transfer to large organic molecules.

In both long and short-range interactions, energy transfer probabilities of the ring CH modes at $\theta = 69.89°$ are now larger than those of the $\theta = 48.60°$ and 98.56° cases, rather than taking values between the two limiting cases. In the long-range interaction model, the ν_3, ν_2 and ν_1 ring-mode probabilities $\theta = 69.89°$ are 0.00746, 0.00611, and 0.00343. At $\theta = 48.60°$ and 98.56°, the corresponding three probabilities are (0.00446, 0.00362 and 0.00198) and (0.00342, 0.00278 and 0.00155). At long range, the ν_3 ring-mode probability is now larger than ν_{17} methyl-mode probability (0.00746 versus 0.00620) despite the situation that the former mode is associated with the energy mismatch twice the latter. Thus, for different groups of modes, a rigorous comparison of energy transfer probabilities cannot be made solely based on the magnitude of the energy mismatch. As shown in Table 1, the perturbation energy of the ring modes is greater than that of the methyl modes at the same distance. At $\theta = 69.89°$, the θ', ϕ-averaged perturbation energies are $\bar{U}_1'(x,\theta) = D[0.4316e^{(x_e-x)/a} - 2(0.0231)e^{(x_e-x)/2a}](x_1\xi/a^2)$ for the ring modes and $\bar{U}_2'(x,\theta) = D[0.1732e^{(x_e-x)/a} - 2(0.0039)e^{(x_e-x)/2a}](x_2\xi/a^2)$ for the methyl modes. Thus, in the representative configuration, DF perturbs the ring modes more strongly than the methyl modes. This greater perturbation energy is responsible for the ring modes leading to larger energy transfer probabilities. Even in the short-range interaction model, the ν_3

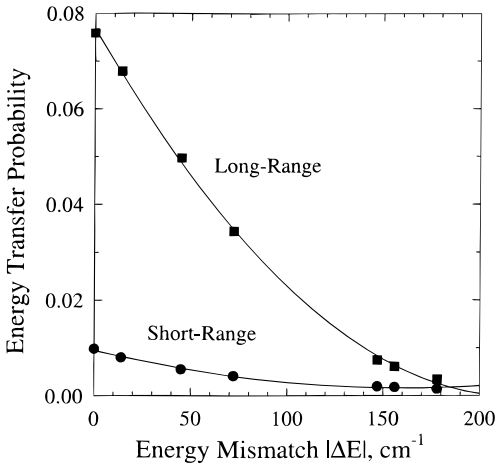

Figure 5. Variation of long-range and short-range energy transfer probabilities for the ring modes in the representative configuration $\theta = 69.89°$. The points at $|\Delta E| = 147$, 156, and 178 cm^{-1} are reproduced from Figure 3b. For the points at the lower values of $|\Delta E|$, the ν_3 frequency is charged toward the DF frequency to alter the energy resonance from -147 cm^{-1} to the resonance case. The four points at $|\Delta E| = 72$, 45, 14, and 0 cm^{-1} in both long and short-range interactions are obtained from such frequency alteration.

probability is larger than the ν_{17} probability (0.0019 versus 0.00071). The results plotted in Figure 3b show that the ring modes, especially the ν_3 mode, can now compete with the methyl modes in deactivating DF(1) at long range. We look into this possibility below.

E. Competition between the Ring and Methyl CH Modes. In Figure 3b for $\theta = 69.89°$, we notice a rapid rise of long-range energy transfer probability from the ν_1 to ν_3 ring CH values and the ν_3 probability is greater than the ν_{17} probability of the methyl CH. This trend indicates that the probability would continue to rise, well above the methyl mode values, if the vibrational frequency of the various ring stretches is changed to alter the energy resonance toward the exact resonance case. To study energy transfer to the ring CH modes in near resonance with DF(1), we choose one of the ring CH modes, for example, the ν_3 mode and alter its energy mismatch to hypothetical values of -72, -45 and -14 cm^{-1}. These values are chosen for convenience as they correspond to the ν_{17}, ν_{28} and ν_4 methyl CH modes, so we can make a direct comparison of the energy transfer efficiencies of the ring modes with those of the methyl modes. In particular, we discuss the details of the $\Delta E = -14$ cm^{-1} case, the lowest energy mismatch that the methyl CH vibration can take. By altering the ν_3 energy mismatch of -147 cm^{-1} down to this value, we can rigorously study competition between ring and methyl modes. Energy transfer probabilities for these altered values of energy mismatch for the ring modes are shown in Figure 5 along with the points for $\Delta E = -147$, -156, and -178 cm^{-1} which are reproduced from Figure 3b. The probabilities calculated in the long-rang interaction model sharply rise when the energy mismatch is lowered below the ν_3 value of -147 cm^{-1}. When $\Delta E = -14$ cm^{-1}, it is as large as 0.0678, which is well above the ν_4 methyl CH probability of 0.0125 obtained in the same long-range model. We note that when the ν_3 frequency is changed to satisfy the exact resonant condition ($\Delta E = 0$), the process is pure VV energy exchange and the probability is 0.0759. On the other hand, a similar application of the ring mode calculation to the energy mismatch below -147 cm^{-1} in the short-range interaction yields energy transfer probabilities which are much less than the long-range values (see Figure 5). Thus, if the ring CH vibration is tuned from the ν_3 frequency toward 2907 cm^{-1} of DF, it can become the principal pathway for deactivating DF(1).

In the present representative configuration, DF approaches toluene along the mid-way line between the ring and methyl CH bonds. In contrast to the $\theta = 98.56°$ case, DF is now away from the "hard-core" interaction region of the benzene ring and maintains an optimal separation from both ring and methyl CH modes to transfer energy from DF(1). The perturbation energy coefficients $A_1'(\theta)$ and $B_1'(\theta)$ of $\theta = 69.89°$ are now larger than those of the $\theta = 98.56°$ case (see Table 1). In this configuration, the efficiency of energy transfer is sensitively dependent on the magnitude of ΔE. Thus, when the ring CH modes are in near resonance with DF(1), energy transfer probabilities become particularly large as shown in Figure 5. The calculation shows the intrinsic preference for energy transfer from the incident molecule to the ring modes in this configuration.

The above results for the representative configuration indicate that of the six CH modes considered, the ν_4 mode of the methyl CH vibration, whose frequency is closest to that of DF, is most efficient in deactivating DF(1). Since the change of quantum numbers is the same ($\Delta v = 2$) for all energy transfer pathways, the factor that mainly controls the present intermolecular VVT energy transfer process *in the given group of modes* is, therefore, the magnitude of energy mismatch. When we want to make a direct comparison between the two different groups, namely the methyl and ring CH modes, it is necessary to bring their energy mismatch to a comparable range. A sharp discontinuity between long-range energy transfer probabilities of the methyl and ring groups seen in Figure 3b clearly indicates a strong tendency of the ring CH bond becoming an efficient energy acceptor. Thus, as shown in Figure 5, when the vibrational frequency of a ring CH mode (e.g., the ν_3 mode) is tuned to alter the energy resonance toward the resonant case, the ring mode can effectively compete with the near-resonant methyl modes in deactivating DF(1). In fact, the present study for the representative configuration shows that in near-resonant collisions, energy transfer to such a ring mode becomes the principal pathway for the deactivation of DF(1). When its frequency is tuned to alter ΔE to -14 cm^{-1}, the ν_3 ring CH mode becomes more than five times as efficient as the ν_4 methyl mode in deactivating DF(1).

IV. Temperature Dependence

All results presented above are calculated at 300 K. As temperature is changed, a significant variation in energy transfer probabilities can occur, even though the energy mismatch is small, because of the effect of the thermal average introduced in eq 10. To discuss this aspect, we take energy transfer to the ν_4 methyl CH mode in the representative configuration. Figure 6a shows the temperature dependence of the ν_4 probability calculated at long range. The result indicates a negative temperature dependence, which is well-known for long-range VV energy transfer processes.[6] The probability is 0.0146 at 100 K and decreases to 0.00840 at 1000 K. At 300 K, it is 0.0125 as already shown in Figure 3b. We note that when the ν_3 energy mismatch is altered to -14 cm^{-1}, the probability at 100 K is as large as 0.0791, far above the ν_4 value. Even at 1000 K, the probability of this altered energy mismatch case is 0.0452. Thus, the discussion presented in the above section on the efficiency of long-range interaction for the ν_3 pathway remains unchanged.

When the short-range interaction model is used, the energy transfer probability now increases with rising temperature, which is the manifestation of short-range interactions (see Figure 6b). In this model, the energy transfer probability is only 0.00058

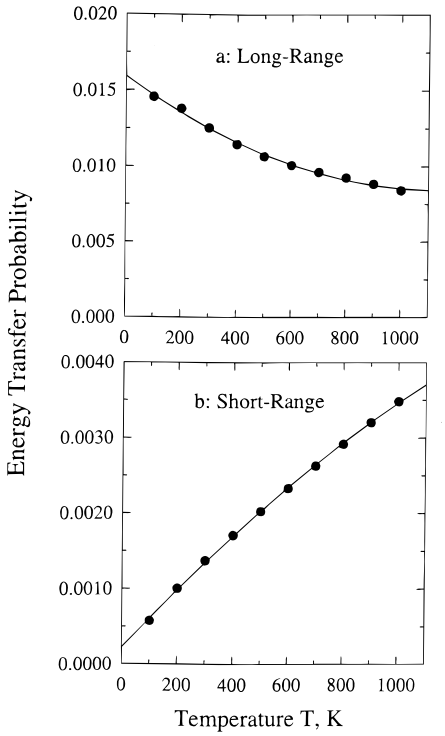

Figure 6. Temperature dependence of the energy transfer probability for the ν_4 methyl CH mode calculated in the (a) long-range interaction model and (b) the short-range interaction model.

at 100 K, but rises to 0.0035 at 1000 K. At 300 K, the probability is 0.0014. These values are far less than the corresponding values obtained in the long-range interaction model. As shown in Figure 6b, the temperature dependence is nearly linear. In the ν_4 process, the energy mismatch is only -14 cm^{-1}. When it is large, however, the increase of energy transfer probabilities with rising temperature in the short-range repulsive model becomes steeper. In such a case, the resulting short-range probability tends to follow the well-known Landau−Teller relation in which log $P(T)$ varies linearly with $T^{-1/3}$.[6,45]

V. Concluding Comments

We have studied transfer of vibrational energy from DF(1) to the benzene ring and methyl group CH stretches of toluene in the long and short-range interaction models using the WKB wave functions. The energy transfer is modeled to follow the VVT process in which the VT step carrying the energy mismatch from translation accompanies the VV exchange step. The most efficient energy transfer pathway is the near-resonant vibrational energy transfer to the near-resonant ν_4 methyl CH mode under the influence of long-range inter-action forces acting between DF and toluene. However, when the frequencies of the ring CH stretches are changed such that the energy mismatch can be systematically lowered toward the resonance case, the ring CH modes compete with the methyl modes in deactivating DF(1) and eventually becoming the dominant energy transfer pathway. The same conclusion holds in the temperature of 100 to 1000 K. In this temperature range, long-range probabilities exhibit negative temperature dependence, while short-range probabilities show a positive dependence.

Appendix

In the short-range interaction model, when the exponent of the wave function given in eq 8 is explicitly evaluated, the perturbation integral $F_{if,1}$ takes the form

$$F_{if,1} = -\frac{aD^{1/2}}{2}(E_i^* E_f^*)^{1/2}\int_{y_{t,i}}^{y_u}\frac{(A_1'y - 2B_1')}{(Y_iY_f)^{1/4}}\times$$
$$\exp\left\{\rho\left[Y_f^{1/2} - Y_i^{1/2} - \frac{B}{A^{1/2}}\ln\left\{\frac{Y_f^{1/2} + A^{1/2}y - B/A^{1/2}}{[B^2/A + (E_f^* + U_{DID})/D]^{1/2}}\right\} + \right.\right.$$
$$\frac{B}{A^{1/2}}\ln\left\{\frac{Y_i^{1/2} + A^{1/2}y - B/A^{1/2}}{[B^2/A + (E_i^* + U_{DID})/D]^{1/2}}\right\} + \left(\frac{E_f^* + U_{DID}}{D}\right)^{1/2} a\tan$$
$$\left(\frac{By + (E_f^* + U_{DID})/D}{[(E_f^* + U_{DID})/D]^{1/2}Y_f^{1/2}}\right) - \left(\frac{E_i^* + U_{DID}}{D}\right)^{1/2} a\tan$$
$$\left(\frac{By + (E_i^* + U_{DID})/D}{[(E_i^* + U_{DID})/D]^{1/2}Y_f^{1/2}}\right) - \frac{\pi}{2}\left[\left(\frac{E_f^* + U_{DID}}{D}\right)^{1/2} - \right.$$
$$\left.\left.\left.\left(\frac{E_f^* + U_{DID}}{D}\right)^{1/2}\right]\right]\right\} dy \quad \text{(A1)}$$

where $\rho = 2a(2mD)^{1/2}/\hbar$, $y = e^{(x_e - x)/2a}$, $Y_i = [Ay^2 - 2By - (E_i^* + U_{DID})/D]$, $Y_f = [Ay^2 - 2By - (E_f^* + U_{DID})/D]$, $E_i^* = E(1 - b^2/b^{*2})$ and $E_i^* = E(1 - b^2/b^{*2}) + \Delta E$. The perturbation integral $F_{if,2}$ takes the same expression except that A_1' and B_2' are now replaced by A_2' and B_2'. Note that A, B, A_1' and B_1' stand for $A(\theta)$, $B(\theta)$, $A_2'(\theta)$ and $B_2'(\theta)$, respectively.

In the long-range interaction model, we use the cosine wave function given by eq 9 for the evaluation of the perturbation integrals. When the integral in the cosine function is explicitly evaluated, we find

$$F_{if,1} = -2aD^{1/2}(E_i^* E_f^*)^{1/4}\int_{y_{t,i}}^{y_u}\frac{(A_1'y - 2B_1')}{(Y_iY_f)^{1/4}}\cos\left\{\rho\left[Y_f^{1/2} + \right.\right.$$
$$\frac{B}{A^{1/2}}a\sin\left(\frac{Ay - B}{[B^2 + A(E_f^* + U_{DID})/D]} - \frac{\pi}{2}\right) - \left(\frac{E_f^* + U_{DID}}{D}\right)^{1/2}\times$$
$$\ln\left[\frac{Y_f^{1/2} + [(E_f^* + U_{DID})/D]}{y} + B\left(\frac{D}{E_f^* + U_{DID}}\right)^{1/2}\right] +$$
$$\left.\left.\frac{1}{2}\left(\frac{E_f^* + U_{DID}}{D}\right)^{1/2}\ln\left(A + \frac{B^2D}{E_f^* + U_{DID}}\right)\right]\right\}\cos\left\{\rho\left[Y_i^{1/2} + \right.\right.$$
$$\frac{B}{A^{1/2}}a\sin\left(\frac{Ay - B}{[B^2 + A(E_i^* + U_{DID})/D]} - \frac{\pi}{2}\right) - \left(\frac{E_i^* + U_{DID}}{D}\right)^{1/2}\times$$
$$\ln\left[\frac{Y_i^{1/2} + [(E_i^* + U_{DID})/D]}{y} + B\left(\frac{D}{E_i^* + U_{DID}}\right)^{1/2}\right] +$$
$$\left.\left.\frac{1}{2}\left(\frac{E_i^* + U_{DID}}{D}\right)^{1/2}\ln\left(A + \frac{B^2D}{E_i^* + U_{DID}}\right)\right]\right\} dy \quad \text{(A2)}$$

We note that in this equation Y_i and Y_f now represent $[-Ay^2 + 2By + (E_i^* + U_{DID})/D]$ and $[-Ay^2 + 2By + (E_f^* + U_{DID})/D]$, respectively. The perturbation integral $F_{if,2}$ takes the same expression except that A_1' and B_2' are replaced by A_2' and B_2' as in the above case.

Acknowledgment. The computational part of this research was supported in part by an NSF Advanced Computing Resources grant through the San Diego Supercomputing Center.

References and Notes

(1) Schwartz, R. N.; Slawsky, Z. I.; Herzfeld, K. F. *J. Chem. Phys.* **1952**, *20*, 1591.

(2) Tanczos, F. I. *J. Chem. Phys*. **1956**, *25*, 439.
(3) Cottrell, T. L.; McCoubrey, J. C. *Molecular Energy Transfer in Gases*; Butterworth: London, 1961; experimental data in Chapter 5 and review of theoretical approaches in Chapter 6.
(4) Burnett, G. M., North, A. M. Eds. *Transfer and Storage of Energy by Molecules*; Wiley: New York, 1969; Vol. 2.
(5) Smith, I. W. M. in *Gas Kinetics and Energy Transfer*; Vol. 2, Specialist Periodical Reports; Chemical Society, Burlington House: London, 1977, pp 1−57.
(6) Yardley, J. T. *Introduction to Molecular Energy Transfer*; Academic: New York, 1980.
(7) Orr, B. In *Advances in Vibrational Energy Transfer Involving Large and Small Molecules*; Barker, J. R., Ed.; JAI Press: Greenwich, CT, 1995; Vol. 2A, pp 21−74.
(8) Watson, R. E., Jr.; Flynn, G. W. *Annu. Rev. Phys. Chem*. **1992**, *43*, 559.
(9) Deroussiaux, A.; Lavorel, B. J. *J. Chem. Phys*. **1999**, *111*, 1875.
(10) Islam, M.; Smith, I. W. M. *J. Chem. Phys*. **1999**, *111*, 9296.
(11) Poel, K. L.; Alwahabi, Z. T.; King, K. D. *Chem. Phys*. **1995**, *201*, 263.
(12) Poel, K. L.; Alwahabi, Z. T.; King, K. D. *J. Chem. Phys*. **1996**, *105*, 1420.
(13) Poel, K. L.; Glavan, C. M.; Alwahabi, Z. T.; King, K. D. *J. Phys. Chem. A* **1997**, *101*, 5614.
(14) Catlett, D. L., Jr.; Parmenter, C. S.; Pursell, C. J. *J. Phys. Chem*. **1994**, *98*, 3263.
(15) Catlett, D. L., Jr.; Parmenter, C. S.; Pursell, C. J. *J. Phys. Chem*. **1995**, *99*, 7371.
(16) Mudjijino; Lawrance, W. D. *J. Chem. Phys*. **1996**, *105*, 3019.
(17) Mudjijino; Lawrance, W. D. *J. Chem. Phys*. **1998**, *109*, 6736.
(18) Toselli, B. T.; Baker, J. R. *J. Chem. Phys*. **1991**, *95*, 8108.
(19) Miller, L. A.; Cook, C. D.; Baker, J. R. *J. Chem. Phys*. **1996**, *105*, 3012.
(20) Shin, H. K. *Chem. Phys. Lett*. **1997**, *281*, 175.
(21) Shin, H. K. *J. Phys. Chem. A* **1999**, *103*, 6030.
(22) Elioff, M. S.; Fraelich, M.; Samson, R. L.; Mullin, A. S. *J. Chem. Phys*. **1999**, *111*, 3517.
(23) Herzberg, C. *Electronic Spectra and Electronic Structure of Polyatomic Molecules*; Van Nostrand: Princeton, NJ, 1967.
(24) Huber, K. P.; Herzberg, G. *Constants of Diatomic Molecules*; Van Nostrand Reinhold: New York, 1979.
(25) Shimanouchi, T. *Tables of Molecular Vibrational Frequencies*; Vol. I, Natl. Stand Ref. Data Ser., Natl. Bur. Stand. No. 39; U.S. Gov. Printing Office: Washington, DC, 1972.
(26) Takayanagi, K. *Prog. Theor. Phys*. **1952**, *8*, 497.
(27) West, R. C. Ed.; *Handbook of Chemistry and Physics*, 60th ed.; CRC Press: Boca Raton, FL, 1979; see p F-216 for bond distances and E-63 for dipole moments.
(28) Hirschfelder, J. O.; Curtiss, C. F.; Bird, R. B. *Molecular Theory of Gases and Liquids*; Wiley: New York, 1967; see pp 1110−1112 and 1212−1214 for D and σ, and pp 949−951 for polarizabilities.
(29) Shin, H. K. *Chem. Phys. Lett*. **1971**, *10*, 81.
(30) Bott, J. F.; Cohen, N. 161st National Meeting of the American Chemical Society, Los Angeles, CA, 1971; Phys. Chem. Paper No. 122.
(31) Pimentel, G. C.; McClellan, A. L. *The Hydrogen Bond*; Freeman: San Francisco, CA, 1960; p 363.
(32) Calvert, J. B.; Amme, R. C. *J. Chem. Phys*. **1966**, *45*, 4710.
(33) Widom, B. *J. Chem. Phys*. **1957**, *27*, 940.
(34) Shin, H. K. *J. Chem. Phys*. **1968**, *49*, 3964.
(35) Child, M. S. *Molecular Collision Theory*; Academic: New York, 1974; Chapter 7.
(36) Landau, L. D.; Lifshits, E. M. *Quantum Mechanics*; Pergamon: London, 1958; pp 178−182.
(37) Rapp, D. *Vibrational Energy Exchange in Quantum and Classical Mechanics*, Technical Report 6-90-61-14; Physics, Lockheed Aircraft Corp.: Sunnyvale, CA, July, 1960.
(38) Widom, B. *Dicuss. Faraday Soc*. **1962**, *33*, 37.
(39) Shin, H. K. *J. Chem. Phys*. **1965**, *42*, 59.
(40) Medvedev, E. S. *Teor. Mater. Fiz*. **1992**, *90*, 218 (Engl. Transl.: *Theor. Math. Phys*. **1992**, *90*, 146).
(41) Nikitin, E. E.; Noda, C.: Zare, R. N. *J. Chem. Phys*. **1993**, *98*, 46.
(42) Karni, Y.; Nikitin, E. E. *J. Chem. Phys*. **1994**, *100*, 2027 and 8065.
(43) Bonemann, F. A.; Nettesheim, P.; Schutte, C. *J. Chem. Phys*. **1996**, *105*, 1074.
(44) Marrison, V. J.; Laposa, J. D. *Spectrochm. Acta* **1976**, *32A*, 443.
(45) Landau, L.; Teller, E. *Phys. Z. Sow*. **1936**, *10*, 34.